ScientificScholar®
Knowledge is power
Publisher of Scientific Journals

www.surgicalneurologyint.com

Surgical Neurology International

Editor-in-Chief: Nancy E. Epstein, MD, Clinical Professor of Neurological Surgery, School of Medicine, State U. of NY at Stony Brook.

SNI: Pediatric Neurosurgery

Editor
Frank Van Calenbergh, MD
University Hospitals; Leuven, Belgium

SNI
Open Access

Case Report

Retained medullary cord and caudal lipoma with histopathological presence of terminal myelocystocele in the epidural stalk

Ai Kurogi[1], Nobuya Murakami[1], Satoshi O. Suzuki[2], Takafumi Shimogawa[3], Nobutaka Mukae[4], Koji Yoshimoto[3], Takato Morioka[5]

[1]Department of Neurosurgery, Fukuoka Children's Hospital, Fukuoka, [2]Department of Psychiatry, Shourai Hospital, Karatsu, [3]Department of Neurosurgery, Kyushu University, Fukuoka, [4]Department of Neurosurgery, Iizuka Hospital, Iizuka, [5]Department of Neurosurgery, Hachisuga Hospital, Munakata, Japan.

E-mail: *Ai Kurogi - kurogi.a@fcho.jp; Nobuya Murakami - murakami.n@fcho.jp; Satoshi O. Suzuki - sosuzuki@shouraikai.jp; Takafumi Shimogawa - shimogawa28@gmail.com; Nobutaka Mukae - mukaen0203@gmail.com; Koji Yoshimoto - yoshimoto.koji.315@m.kyushu-u.ac.jp; Takato Morioka - takatons1227@gmail.com

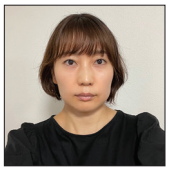

***Corresponding author:**
Ai Kurogi,
Department of Neurosurgery,
Fukuoka Children's Hospital,
Fukuoka, Japan.

kurogi.a@fcho.jp

Received : 05 June 2023
Accepted : 14 July 2023
Published : 04 August 2023

DOI
10.25259/SNI_479_2023

Quick Response Code:

ABSTRACT

Background: The retained medullary cord (RMC), caudal lipoma, and terminal myelocystocele (TMCC) are thought to originate from the failed regression spectrum during the secondary neurulation, and the central histopathological feature is the predominant presence of a central canal-like ependyma-lined lumen (CC-LELL) with surrounding neuroglial tissues (NGT), as a remnant of the medullary cord. However, reports on cases in which RMC, caudal lipoma, and TMCC coexist are very rare.

Case Description: We present two patients with cystic RMC with caudal lipoma and caudal lipoma with an RMC component, respectively, based on their clinical, neuroradiological, intraoperative, and histopathological findings. Although no typical morphological features of TMCC were noted on neuroimaging, histopathological examination revealed that a CC-LELL with NGT was present in the extraspinal stalk, extending from the skin lesion to the intraspinal tethering tract.

Conclusion: This histopathological finding indicates the presence of TMCC that could not be completely regressed and further supports the idea that these pathologies can be considered consequences of a continuum of regression failure during secondary neurulation.

Keywords: Caudal lipoma, Closed spinal dysraphism, Epidural stalk, Retained medullary cord, Secondary neurulation failure, Terminal myelocystocele

INTRODUCTION

Although the precise mechanism of the secondary neurulation remains unknown, it is generally speculated that it begins with mesenchymal epithelium transformation within a pluripotent blastema called the caudal cell mass.[2,5,11,17,20,24] A sequence of events then proceeds from the condensation of the mesenchyme into a solid medullary cord (condensation phase) to intrachordal lumen formation (cavitation and canalization phases) and eventual partial regression of the cavitary medullary cord until only the conus below the S1 and S2 and filum remain (regression phase).

The retained medullary cord (RMC) is an entity of closed spinal dysraphism characterized by a redundant nonfunctional "cord-like structure (C-LS)" continuous from the functional conus

and extending to the dural cul-de-sac, which leads to cord tethering.[17,18,20,21] RMC is thought to originate from the failed regression of the medullary cord,[2,17,20,24] and the characteristic histopathological feature is the presence of a central canal-like ependyma-lined lumen (CC-LELL) with surrounding neuroglial tissues (NGT), as a remnant of the medullary cord.[2,4,5,9-12,14-17,20,23] The cyst within the RMC is histopathologically a cystic dilatation of the CC-LELL with NGT, and this pathology is called "cystic RMC."[2-4,14,17,24]

Although diagnostic criteria for RMC have not yet been fully established, the following three items are generally considered important:[11] (1) typical morphological features on neuroimaging and intraoperative view,[2,17,20,24] (2) the electrophysiological border between the conus and C-LS,[2,4,9-12,17,20,21,24] and (3) CC-LELL with NGT on histopathological examination of C-LS.[2,4,9-12,15-17,20,21,23,24] Our recent reports demonstrated that the caudal lipoma fulfilled most of the three items, and RMC and caudal lipoma are thought to exist in the same pathological spectrum of regression failure.[11] The only prominent difference between these two is the difference in the proportions of fibroadipose and fibrocollagenous tissues (FAT and FCT), and it may not be possible to clearly distinguish between the two.[11]

The terminal myelocystocele (TMCC) is an unusual type of closed spinal dysraphism, characterized by cystic dilatation of the terminal portion of the central canal with a trumpet-like configuration that herniates through a spinal bifida.[1,7,8,18,19] In addition, the histopathological features of the TMCC wall are the same as those of RMC. Although the precise embryopathogenesis of TMCC remains obscure, recent authors considered that TMCC is also regression failure at the stage of the persistent terminal balloon, which is normally formed at the distal tip of the medullary cord and destined to detach from the skin and regress.[2,6,18,19,22,24]

Recently, we treated two patients with RMC and caudal lipoma. While no typical morphological features of TMCC were observed on neuroimaging, CC-LELL with NGT was histopathologically recognized in the extraspinal stalk, continuing from the skin lesion to the intraspinal tethering tract, which was suspected to be the coexistence of RMC and TMCC that could not be completely regressed. Here, we report details of clinical, neuroradiological, intraoperative, and histopathological findings of these cases.

CASE REPORT

Patient 1

The boy was detected with an abnormal gluteal cleft at birth and was referred to us at the age of 5 months. A Y-shaped groove continuous from the gluteal cleft was noted [Figure 1a], and a dimple was observed under the groove on the right side [Figure 1b, blue arrow]. No neurological

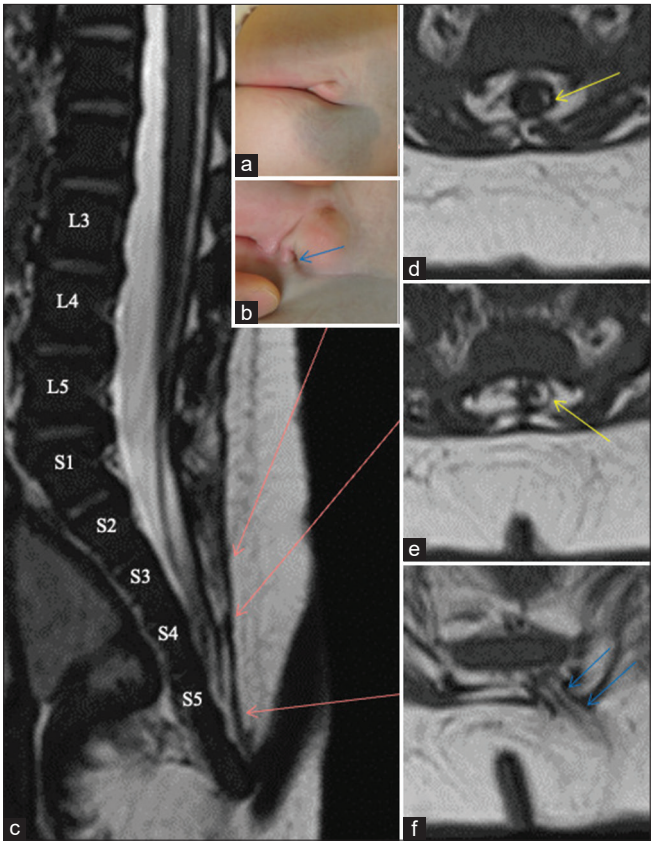

Figure 1: (Patient 1) (a and b) Photographs of the skin lesion, shows a dimple (blue arrows) under the groove on the right side. (c-f) Sagittal view of 3D-hT2WI (c) and axial views of T1WI (d-f). Each slice level of the axial views (d-f) is indicated by red arrows on (c). Each level of the vertebral columns from L3 to S5 is indicated on (c). The caudal cyst wall is partly composed of lipomatous tissue (d,e, yellow arrows). A stalk extending from the subcutaneous fat into the vertebral canal is shown as blue arrows [panel (f)]. 3D-hT2WI: three-dimensional heavily T2-weighted image, T1WI: T1-weighted image.

abnormalities were observed. Magnetic resonance imaging (MRI) revealed the caudal spinal cord and continuous C-LS, with a large cyst at the S1–S3 of the vertebral level, with cord tethering [Figure 1c]. The caudal cyst wall was partly composed of lipomatous tissue [Figures 1d and e; yellow arrows]. At the S5 level, a stalk extending from the subcutaneous fat into the vertebral canal was noted, but there was no cyst indicating TMCC in it [Figure 1f, blue arrows].

We performed untethering surgery at the age of 6 months. A skin incision was made to surround the dimple, and a stalk continuous from the subcutaneous fat entered the spinal canal through the myofascial defect [Figure 2a, blue arrows]. The dural sac was exposed through bifid S1–S5, and the stalk entered the dura at the dural cul-de-sac [Figure 2b]. When the dura was opened, the cyst was visible in the rostral part of the C-LS and the caudal part was a lipoma [Figures 2c and d].

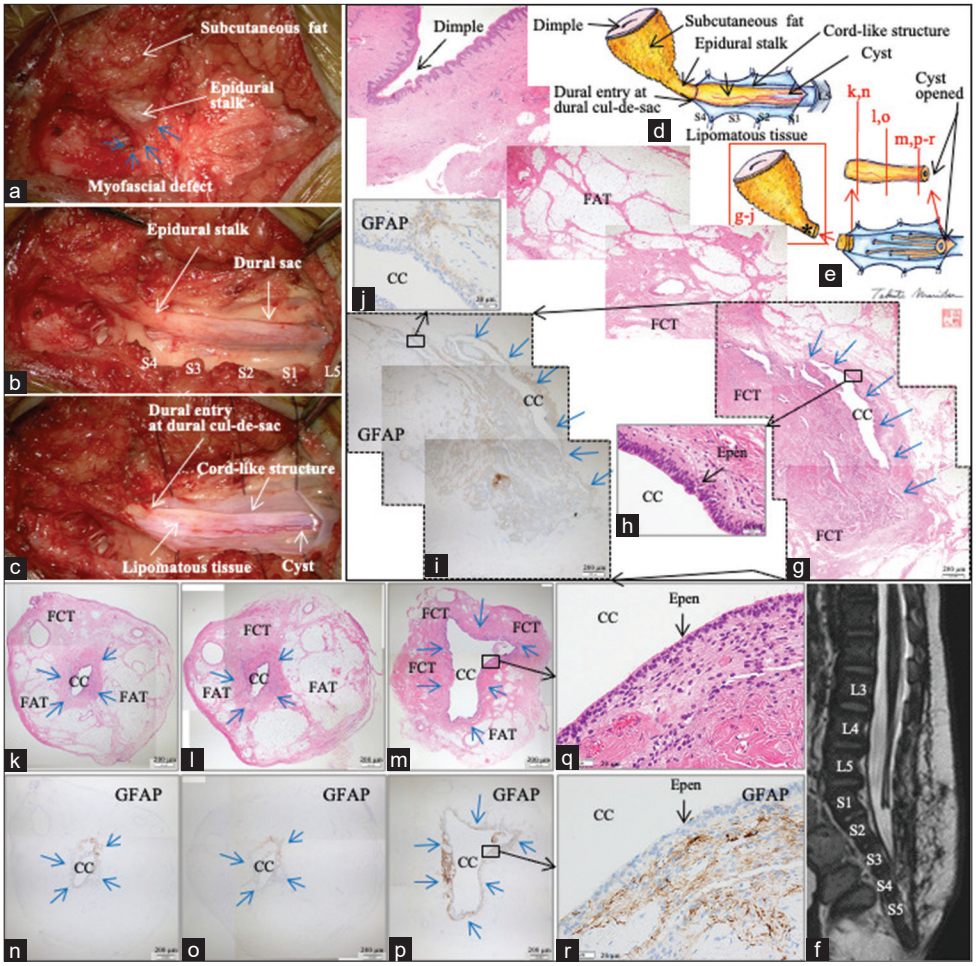

Figure 2: (Patient 1) (a-c) Microscopic views and (d and e) schematic drawings of the operative findings. Each level of the exposed vertebral arches from L5 to S4 is indicated on (b). (f) Sagittal view of postoperative 3D-hT2WI. Each level of the vertebral columns from L3 to S5 is indicated on (f). (g-i) Photomicrographic composite of the vertical view of the skin and epidural stalk, stained with H&E (g and h) and immunostained for GFAP (i and j). (k-r) Photomicrograph of the axial sections of the cord-like structure stained with H&E (k-m and q) and immunostained for GFAP (n-p and r). CC-LELL with NGT is surrounded by blue arrows on (g), (i), and (k-p). The location of each section is indicated as "g-r" in (e). The location of each section is indicated in (e). The location of central canal-like ependyma-lined lumen surrounded by neuroglial tissue in the epidural stalk is indicated as * in (e) and (g-j and k-r). The sites surrounded by dotted line in (g and i) indicate the same site. Higher magnification views of the areas indicated by the square in (g, i, m, and p) are shown in (h, j, q, and r), respectively. 3D-hT2WI, three dimensional heavily T2-weighted image, H&E: hematoxylin and eosin, CC-LELL, central canal-like ependyma-lined lumen; GFAP: glial fibrillary acidic protein, FAT: fibroadipose tissue, FCT: fibrocollagenous tissue, CC: central canal-like structure, and Epen: ependymal cells.

After confirming that the exposed C-LS in the operative field was nonfunctional with intraoperative neurophysiological monitoring (IONM) as previously described,[4,5,9-12,14-16,23] the C-LS with lipomatous tissue was firstly severed near the dural cul-de-sac, and the C-LS rose proximally by approximately 1 cm. When the C-LS was incised at the S2 level, the cyst was opened. The C-LS was resected as column. The epidural stalk was then cut just distal to the dural cul-de-sac and excised together with the skin lesion [Figure 2e].

Postoperatively, no *de novo* neurological abnormalities were observed. MRI performed on the 7th postoperative day demonstrated successful untethering of the cord [Figure 2f]. No remnant cystic cavity or hydromyelia was observed.

Histopathologically, the distal side of the epidural stalk, continuing from the skin dimple, was mainly composed of FAT, while the proximal side was mainly composed of FCT [Figure 2g]. The CC-LELL surrounded by glial fibrillary

acidic protein (GFAP)-positive NGT was observed in FCT on the proximal side [Figures 2e,*,g-j, blue arrows]. The C-LS was composed of FAT, and the component of FCT increased toward the proximal side [Figures 2k-m]. In addition, CC-LELL surrounded by NGT was observed in these tissues [Figures 2k-r, blue arrows], which increased in size toward the proximal side, and exhibited the form of cystic dilation of CC-LELL at the most proximal side [Figures 2m and p].

Patient 2

The boy, with joint contractures in the four limbs due to arthrogryposis multiplex congenita, had an abnormal gluteal cleft with skin lesions at birth [Figure 3a]. MRI at the age of 2 months showed a tethered cord with caudal lipoma and syringomyelia in the cord at the L1- L5 of the vertebral level [Figure 3b], and he was referred to us. Since it was determined that joint contractures were not related to the spinal anomaly, orthopedic treatments, including bilateral Achilles tenotomy, were prioritized, and the patient was transferred to us at 7 months.

Neurologically, there was little movement of the four limbs, and in particular, no movement of the bilateral ankle joints was observed. However, regular urination and defecation were observed. The second MRI revealed that the caudal lipoma increased in size and extension to the subcutaneous fat through an enlarged sacral hiatus became apparent [Figures 3c and d]. There were no morphological features of the TMCC. Thin-sliced sagittal views showed little change in syringomyelia size.

We performed untethering surgery at 7 months. A skin incision was made to surround the skin lesion, and a fatty stalk continuous from the subcutaneous fat entered the spinal canal through the myofascial defect [Figure 3e]. The dural sac was exposed through laminoplastic laminotomy at L5 and bifid S1 to S3, and the epidural lipoma entered the dura at the dural cul-de-sac [Figure 3f]. When the dura was opened, the caudal lipoma and the tethered conus were exposed [Figures 3g and h]. IONM confirmed the existence of an electrophysiological border at the operative microscopic boundary between the two [Figure 3i]. The caudal lipoma was first severed near the dural cul-de-sac. When the lipoma was debulked in the proximal direction, a tiny cyst was exposed. The cyst wall was resected for the histopathological specimen [Figure 3j]. The lipoma was furtherly debulked to near the border with the conus, and the stump was sutured with pial sutures. The epidural lipoma was cut just distal to the dural cul-de-sac and excised together with the skin lesion [Figure 3j].

Postoperatively, no *de novo* neurological abnormalities were observed. MRI performed on the 7th postoperative day demonstrated successful untethering of the cord [Figure 3k]. No change in syringomyelia size was observed.

Histopathologically, the skin lesion contained clusters of blood vessels beneath the squamous epithelium [Figure 3l, red square] and was diagnosed as angioma. The epidural fatty stalk, continuing from the skin angioma, was mainly composed of FAT [Figure 3l]. In the FAT of the proximal side, CC-LELL surrounded by GFAP-positive NGT was observed [Figures 3j, *, l and m, blue arrows, n and o]. The intradural lipoma was typically composed of FAT. The cyst wall in the lipoma had NGT surrounded by the FCT in the FAT, whereas no CC-LELL was noted [Figures 3p and q, blue arrows].

DISCUSSION

The C-LS of Patient 1 satisfied items (1) and (3) of the three items for diagnosing RMC.[11] However, although we did not perform additional invasive laminotomy to fully satisfy item (2), we confirmed that the C-LS in the exposed area was electrophysiologically nonfunctional. Therefore, the C-LS in this case was diagnosed as RMC. In addition, because the cyst within the RMC was histopathologically a cystic dilatation of the CC-LELL with NGT and had lipomatous component, the final diagnosis of cystic RMC with caudal lipoma was made based on our previous report.[4,11,14]

In Patient 2, the caudal lipoma was tethered to the spinal cord, and the electrophysiological border was identified at the morphological border between the two. There was a tiny cyst within the lipoma, and there was GFAP-positive NGT in its wall. Since the CC-LELL was not entirely included in the specimen,[9-12] we assumed that their presence could not be proven and the diagnosis of caudal lipoma with RMC component was finally made also based on our previous report.[4,11,14]

The most prominent histopathological finding of the epidural stalk in the present cases was that the CC-LELL surrounded by NGT, which is also a characteristic finding of TMCC, was observed in the FCT, while no typical morphological features of TMCC were noted on neuroimaging. Direct communication between the CC-LELL and RMC has not been histopathologically proven. However, because the CC-LELL was located on the proximal side of the epidural stalk, it is possible that there was an originally communication between them. Therefore, this histopathological finding indicates the presence of TMCC that could not be completely regressed and supports the idea raised by previous authors that TMCC and RMC can be considered consequences of a continuum of regression failure during secondary neurulation.[2,3,18,19,22,24]

However, reports of cases in which RMC and TMCC coexist are extremely rare. To date, only three cases have been reported. Kim *et al*.[3] reported a case in which cystic

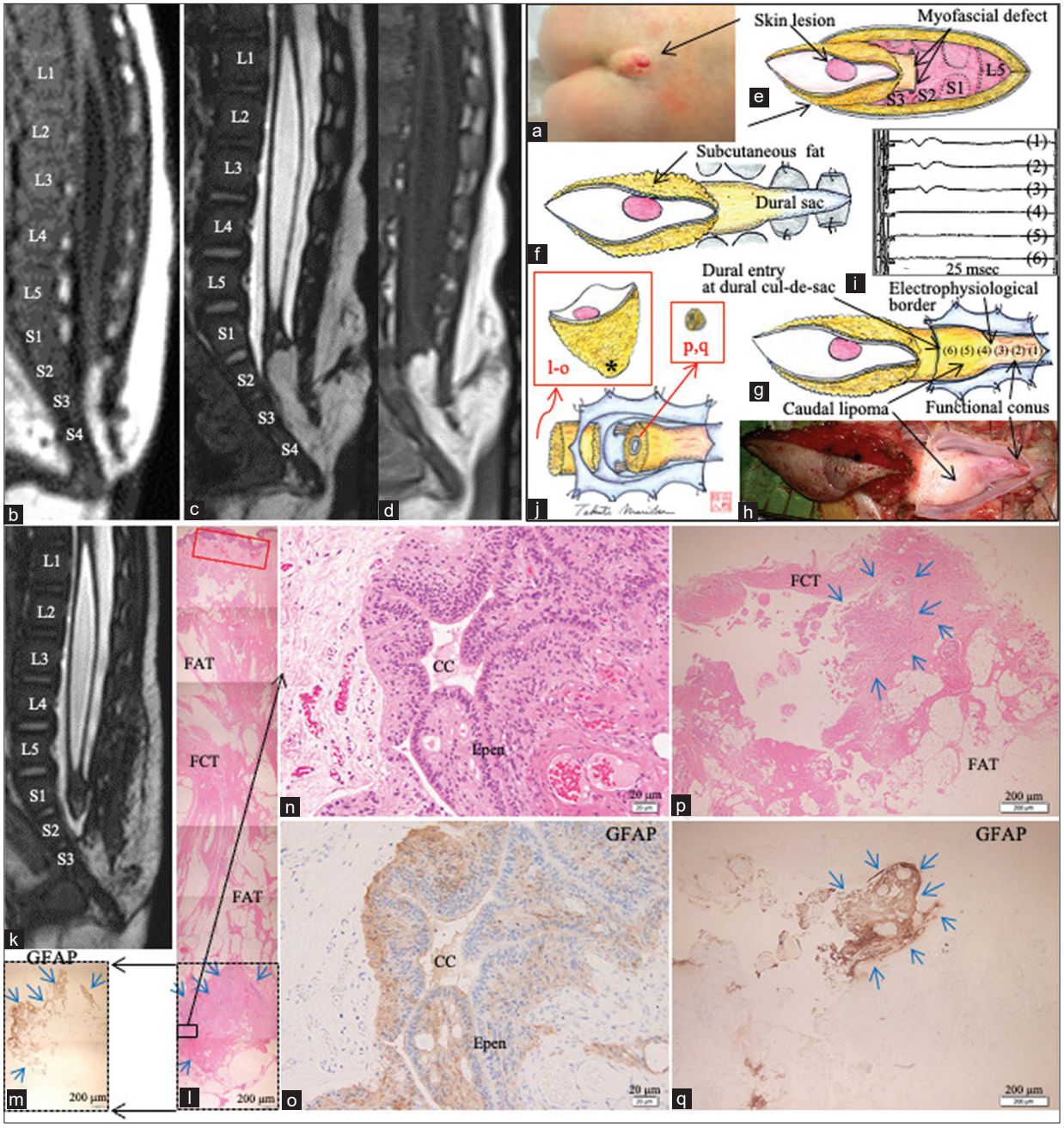

Figure 3: (Patient 2) (a) Photograph of the skin lesion. (b) Sagittal view of T1WI at the age of 2 months, (c and d) sagittal views of 3D-hT2WI (c) and T1WI (d) at the age of 7 months. Each level of the vertebral columns from L3 to S5 is indicated on (b) and (c). and (e-i) Schematic drawings (e-g and i) and microscopic view (h) of the operative findings. (j) The electrophysiological border between functional conus and caudal lipoma was determined with IONM, by tracing the evoked compound muscle potentials of the external anal sphincter with stimulation of 2 mA, beginning from the functional conus (g-(1)(2)(3)), and proceeding to the caudal lipoma (g-(4)(5)(6)). Stimulation sites are indicated on (g). Each histopathology section is shown in red characters "l-o, p/q". (k) Sagittal view of postoperative 3D-hT2WI. (l-o) Photomicrographic composite of the vertical view of the skin and epidural stalk, stained with H&E (l and n) and immunostained for GFAP (m and o). CC-LELL with NGT is surrounded by blue arrows on (m), (l), (p), and (q). The location of CC-LELL with NGT surrounded by neuroglial tissue in the epidural stalk is indicated as * in (j). The sites surrounded by dotted line in (l and m) indicate the same site. Higher magnification views of the area indicated by the square in (l) are shown in (n and o), respectively. (p and q) Photomicrograph of the cyst wall in the lipoma stained with H&E (p) and immunostained for GFAP (q). The location of each section is indicated as l-o and p, q in (j). T1WI: T1-weighted image, 3D-hT2WI: three-dimensional heavily T2-weighted image, IONM: Intraoperative neurophysiological monitoring, H&E: hematoxylin and eosin, CC-LELL, central canal-like ependyma-lined lumen; GFAP: glial fibrillary acidic protein, FAT: fibroadipose tissue, FCT: fibrocollagenous tissue, cc: central canal-like structure, and Epen: ependymal cells.

RMC in a J-shaped cul-de-sac extended to an extradural cyst with glioependymal lining. Shim *et al*.[22] reported an RMC with cystic dilatation of the caudal end extending to the epidural cyst resembling a TMCC. We reported a baby girl with a huge sacrococcygeal meningocele-like sac with two components.[5] RMC and associated intramedullary arachnoid cyst were terminated at the bottom of the rostral cyst, forming the septum of the two cystic components, and the caudal cyst was TMCC derived from CC-LELL of the RMC at the septum.

The most likely reason why the histopathological coexistence of TMCC and RMC tissues has rarely been reported, as in these cases, is that the tethering tract caused by secondary neurulation failures, such as RMC and caudal lipoma, is rarely continuous from the skin lesion to the spinal canal through the myofascial defect and spina bifida,[13] unlike the primary neurulation failure, and few histopathological studies on the epidural stalk have been performed. Both patients in the present study had a continuous tract from the skin lesion to the spinal canal through a myofascial defect and sacral hiatus. The CC-LELL with NGT is also a characteristic histopathological finding of the stalks in limited dorsal myeloschisis (LDM).[9] However, LDM is caused by primary neurulation failure,[9] and there is no possibility of merging at the dural cul-de-sac.

Untethering of the cord was the best surgical method for both patients. Another important issue is the surgical strategy used to treat cystic lesions. In Patient 1, the cyst was present in the nonfunctional RMC; therefore, untethering was performed at the site of the cystic RMC, which directly opened the cyst, leading to postoperative reduction in its size as previously reported.[4,14] In Patient 2, the cyst (syringomyelia) was present in the functional cord at the central side of the caudal lipoma and was asymptomatic; therefore, no surgical treatment was performed. Thus, the long-term follow-up is necessary in the future.

Furthermore, an active histopathological search of the epidural stalk revealed a small TMCC tissue. Future studies are expected to increase the number of cases with coexistence of TMCC and RMC.

CONCLUSION

This histopathological finding indicates the presence of TMCC that could not be completely regressed and further supports the idea that these three pathologies can be consequences of a continuum of regression failure during secondary neurulation.

Declaration of patient consent

The authors certify that they have obtained all appropriate patient consent.

Financial support and sponsorship

Research Foundation of Fukuoka Children's Hospital.

Conflicts of interest

There are no conflicts of interest.

REFERENCES

1. Hashiguchi K, Morioka T, Samura K, Yoshida F, Miyagi Y, Nagata S, *et al*. Holocord hydrosyringomyelia with terminal myelocystocele revealed by constructive interference in steady-state MR imaging. Pediatr Neurosurg 2008;44:509-12.
2. Kim KH, Lee JY, Wang KC. Secondary neurulation defects-1: Retained medullary cord. J Korean Neurosurg Soc 2020;63:314-20.
3. Kim KH, Lee JY, Yang J, Park SH, Kim SK, Wang KC. Cystic retained medullary cord in an intraspinal J-shaped cul-de-sac: A lesion in the spectrum of regression failure during secondary neurulation. Childs Nerv Syst 2021;37:2051-6.
4. Kurogi A, Murakami N, Morioka T, Mukae N, Shimogawa T, Kudo K, *et al*. Two cases of retained medullary cord running parallel to a terminal lipoma. Surg Neurol Int 2021;12:112.
5. Kurogi A, Murakami N, Mukae N, Shimogawa T, Shono T, Suzuki SO, *et al*. Retained medullary cord associated with terminal myelocystocele and intramedullary arachnoid cyst. Pediatr Neurosurg 2022;57:184-90.
6. Lee JY, Kim SP, Kim SW, Park SH, Choi JW, Phi JH, *et al*. Pathoembryogenesis of terminal myelocystocele: Terminal balloon in secondary neurulation of the chick embryo. Childs Nerv Syst 2013;29:1683-8.
7. McLone DG, Naidich TP. Terminal myelocystocele. Neurosurgery 1985;16:36-43.
8. Morioka T, Hashiguchi K, Yoshida F, Matsumoto K, Miyagi Y, Nagata S, *et al*. Neurosurgical management of occult spinal dysraphism associated with OEIS complex. Childs Nerv Syst 2008;24:723-9.
9. Morioka T, Murakami N, Ichiyama M, Kusuda T, Suzuki SO. Congenital dermal sinus elements in each tethering stalk of coexisting thoracic limited dorsal myeloschisis and retained medullary cord. Pediatr Neurosurg 2020;55:380-7.
10. Morioka T, Murakami N, Kanata A, Tsukamoto E, Suzuki SO. Retained medullary cord with sacral subcutaneous meningocele and congenital dermal sinus. Childs Nerv Syst 2020;36:423-7.
11. Morioka T, Murakami N, Kurogi A, Mukae N, Shimogawa T, Shono T, *et al*. Embryopathological relationship between retained medullary cord and caudal spinal lipoma. Interdiscip Neurosurg 2022;29:101534.
12. Morioka T, Murakami N, Suzuki SO, Mukae N, Shimogawa T, Kurogi A, *et al*. Surgical histopathology of a filar anomaly as an additional tethering element associated with closed spinal dysraphism of primary neurulation failure. Surg Neurol Int 2021;12:373.
13. Morota N, Ihara S, Ogiwara H. New classification of spinal lipomas based on embryonic stage. J Neurosurg Pediatr 2017;19:428-39.

14. Mukae N, Morioka T, Suzuki SO, Murakami N, Shimogawa T, Kanata A, *et al*. Two cases of large filar cyst associated with terminal lipoma: Relationship with retained medullary cord. World Neurosurg 2020;142:294-8.
15. Murakami N, Morioka T, Shimogawa T, Hashiguchi K, Mukae N, Uchihashi K, *et al*. Retained medullary cord extending to a sacral subcutaneous meningocele. Childs Nerv Syst 2018;34:527-33.
16. Murakami N, Morioka T, Shimogawa T, Mukae N, Inoha S, Sasaguri T, *et al*. Ependyma-lined canal with surrounding neuroglial tissues in lumbosacral lipomatous malformations: Relationship with retained medullary cord. Pediatr Neurosurg 2018;53:387-94.
17. Pang D, Chong S, Wang KC. Secondary neurulation defects-1: Thickened filum terminale, retained medullary cord. In: Di Rocco C, Pang D, Rutka J, editors. Textbook of Pediatric Neurosurgery. 1st ed. Switzerland: Springer; 2020a.
18. Pang D, Lee JY, Wang KC. Secondary neurulation defects-2: Terminal myelocystocele: Surgical observations, laboratory findings, and theory of embryogenesis. In: Di Rocco C, Pang D, Rutka JT, editors. Textbook of Pediatric Neurosurgery, 1st ed. Switzerland, Springer; 2020b.
19. Pang D, Zovickian J, Lee JY, Moes GS, Wang KC. Terminal myelocystocele: Surgical observations and theory of embryogenesis. Neurosurgery 2012;70:1383-405; discussion 1404-5.
20. Pang D, Zovickian J, Moes GS. Retained medullary cord in humans: Late arrest of secondary neurulation. Neurosurgery 2011;68:1500-19; discussion 1519.
21. Sala F, Barone G, Tramontano V, Gallo P, Ghimenton C. Retained medullary cord confirmed by intraoperative neurophysiological mapping. Childs Nerv Syst 2014;30:1287-91.
22. Shim Y, Park HJ, Kim KH, Park SH, Wang KC, Lee JY. Retained medullary cord and terminal myelocystocele as a spectrum: Case report. Childs Nerv Syst 2022;38:1223-8.
23. Shirozu N, Morioka T, Inoha S, Imamoto N, Sasaguri T. Enlargement of sacral subcutaneous meningocele associated with retained medullary cord. Childs Nerv Syst 2018;34:1785-90.
24. Yang J, Lee JY, Kim KH, Wang KC. Disorders of secondary neurulation: Mainly focused on pathoembryogenesis. J Korean Neurosurg Soc 2021;64:386-405.

How to cite this article: Kurogi A, Murakami N, Suzuki SO, Shimogawa T, Mukae N, Yoshimoto K, *et al.* Retained medullary cord and caudal lipoma with histopathological presence of terminal myelocystocele in the epidural stalk. Surg Neurol Int 2023;14:279.